

Electronic structure and rebonding in the onion-like $\text{As@Ni}_{12}@As_{20}$ cluster

Tunna Baruah^{1,4}, Rajendra R. Zope², Steven L. Richardson^{3,4}, and Mark R. Pederson⁴

¹*Department of Physics, Georgetown University, Washington DC, 20057*

²*School of Computational Sciences, George Mason University, Fairfax, VA 22030*

³*Department of Electrical Engineering and Materials Science Research Center, Howard University, School of Engineering, Washington, DC 20059 and*

⁴*Center for Computational Materials Science, Naval Research Laboratory, Washington DC 20375-5345*

(Dated: November 2, 2018)

We present the first *ab initio* study of the geometry, electronic structure, charged states, bonding and vibrational modes of the recently synthesized fullerene-like $\text{As@Ni}_{12}@As_{20}$ cluster which has icosahedral point symmetry [Science, **300**, 778 (2003)]. We show that the molecule is vibrationally stable and will be electronically most stable in its -3 oxidation state in the condensed phase and in -2 state in the gas phase. We examine the bonding in this unusually structured molecule from charge transfer between atoms, infrared and Raman spectra, and charge density isosurfaces.

PACS numbers: 36.40.Cg, 36.40.Mr, 36.40.Qv, 31.40.+z

Keywords: fullerene, Infrared, Raman, electronic structure, vibration, polarizability

Since the discovery that carbon can form fullerene-like structures of high symmetry [1, 2], there has been considerable speculation, both experimentally and theoretically, as to whether symmetric fullerene-like clusters can be created from other elements [3, 4]. Solids comprised of such inorganic sub-units can have important applications in nanotechnology and materials science. An important step towards this goal was realized with the recent synthesis of the $[(C_4H_9)_4P^{+1}]_3[As@Ni_{12}@As_{20}]^{-3}$ salt by Moses *et al.* [5] where the $[As@Ni_{12}@As_{20}]^{-3}$ anion (Cf. Fig. 1a) is comprised of an icosahedral (I_h) $As@Ni_{12}$ cluster with an arsenic atom core (Cf. Fig. 1b) encapsulated by a dodecahedral fullerene-like As_{20} cage (Cf. Fig. 1c) to give an onion-skin-like $[As@Ni_{12}@As_{20}]^{-3}$ cluster with icosahedral point symmetry. As discussed by Moses *et al.* [5], clusters with this structure form the inner core of a class of intermetallic compounds which were first identified by Bergman *et al.* [6]. Such cores might actually be responsible for the formation of quasicrystals. The encapsulating As_{20} shows only structural resemblance to a carbon-based fullerene. Electronically, the atoms in As_{20} are sp^3 -hybridized with three bonding orbitals along the surface of the dodecahedron and a fourth orbital containing a lone pair of electrons pointing outward from the cage. In the carbon-based fullerenes the carbon atoms are sp^2 -hybridized forming a strong covalently-bonded network of σ -bonds surrounded by a sheath of π -electrons in bonding orbitals.

The $As@Ni_{12}@As_{20}$ cluster is fascinating in that it represents another example of what Müller has called the “beauty of symmetry” where the interpenetrating nature of the As_{20} dodecahedron and the $As@Ni_{12}$ icosahedron yield a polyhedra of sixty triangular faces [7]. Further, it demonstrates the first experimental confirmation of a completely non-carbon fullerene-like dodecahedron, As_{20} . At this stage, very little is known about the molecule and the only theoretical study to date has calculated the molecular orbital energies with the semi-empirical extended Hückel method [5]. In this commu-

nication, we present results of our first-principles density functional theory (DFT) studies on the isolated neutral and anionic states of the $As@Ni_{12}@As_{20}$ cluster and its sub-units, As_{20} and $As@Ni_{12}$, to determine their respective electronic structure, vibrational stability, and chemical bonding patterns. In particular, our calculations demonstrate that a rehybridization of the the covalent As-As bonds present in the isolated As_{20} cage takes place to form new As-Ni bonds between the inner $As@Ni_{12}$ cluster and the outer As_{20} cage.

Our DFT calculations were performed at the all-electron level with the generalized gradient approximation (GGA) [8] to describe the exchange-correlation effects. We have performed these calculations with T_h symmetry but we find that the optimized geometry has I_h symmetry which was verified from the positions of the atoms. All calculations have been performed using the NRLMOL package [9] which employs a Gaussian basis set where the exponentials are optimized for each atom.

The optimized equilibrium geometries of the isolated $As@Ni_{12}@As_{20}$ molecule along with its two sub-units are shown in Fig. 1. For the free standing icosahedral $As@Ni_{12}$, the core As-Ni distance is 2.36 Å while the Ni-Ni distance is 2.48 Å. In the As_{20} cage, the As-As distance is 2.5 Å which is in good agreement with earlier calcu-

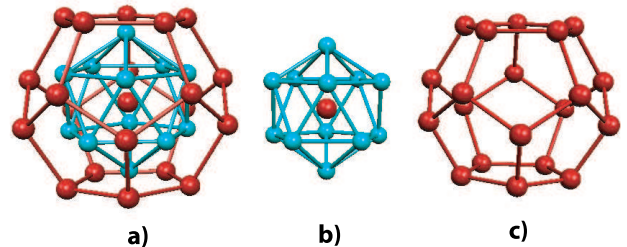


FIG. 1: Structures of a) $As@Ni_{12}@As_{20}$, b) $As@Ni_{12}$, and c) As_{20} .

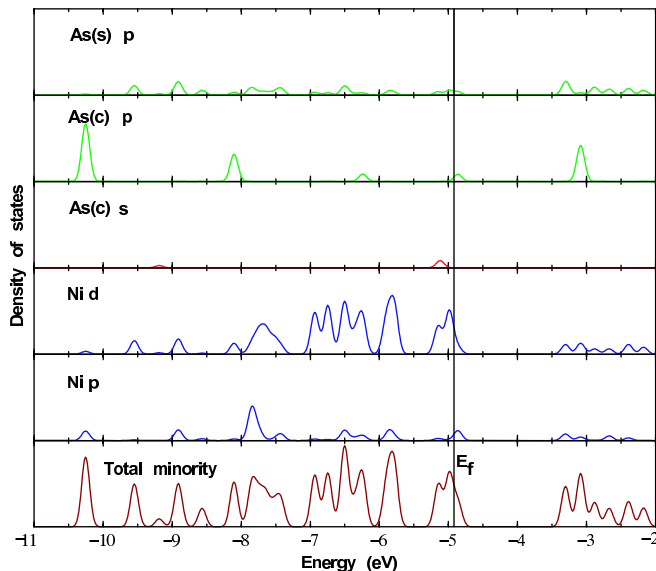


FIG. 2: The total and atom projected partial density of states in arbitrary units of $\text{As@Ni}_{12}\text{@As}_{20}$ of the minority channel. The three upper panel shows the projected density on the central (c) and outer shell (s) As atoms. The Ni p DOS is magnified for presentation purpose.

lated results [10]. Upon formation of the $\text{As@Ni}_{12}\text{@As}_{20}$ structure, the central As-Ni, Ni-Ni, and the outer cage As-As distances increase to 2.61, 2.74, and 2.8 Å, respectively. The Ni to outer layer As distance is 2.43 Å. The interatomic distances increase by about 10-12 % upon formation of the $\text{As@Ni}_{12}\text{@As}_{20}$ molecule as compared to isolated sub-units. These bond lengths are in excellent agreement with the experimental values (Cf. Table I). We note that while our calculated bond lengths are for the neutral molecule, the experimental values are for the molecule in the crystalline environment where it is in -3 charged state and the perfect I_h symmetry is weakly broken by standard crystal field effects and by the positively charged ligands. Our calculations have shown that the structural changes induced by the excess charge are small - from 0.4 to 1 %.

The calculated atomization energy of the free-standing As_{20} unit is 2.79 eV and that of the As@Ni_{12} is 3.05 eV. The $\text{As@Ni}_{12}\text{@As}_{20}$ molecule has atomization energy of 3.7 eV and is stable by about 26 eV with respect to its two sub-units. Its ionization potential is 6.4 eV.

The calculated total and atom projected density of states (DOS) of the isolated neutral molecule are shown in Fig. 2. Since the majority states are completely occupied, we show the DOS for minority states responsible for chemical interaction. Both the highest occupied molecular orbital (HOMO) and the lowest unoccupied molecular orbital belong to the minority states. The HOMO has H_u symmetry, while the LUMO has T_{1u} symmetry. The eigenvalues of HOMO and LUMO along with the Hubbard U values are presented in Table I. The neutral cluster has a spin magnetic moment of $3 \mu_B$. Reduction

to the -3 charged state quenches the magnetic moment and opens up a large HOMO-LUMO gap, as is evident from the Fig. 2. This in turn stabilizes the molecule by 2.4 eV. The HOMO-LUMO gap in the neutral and triply charged state are 0.115 and 1.45 eV, respectively. This observation is in accord with the magnetic susceptibility measurement as well as with the Hückel model prediction [5]. The DOS of the As@Ni_{12} molecule (not shown) shows As s states in the excited levels which become occupied in the $\text{As@Ni}_{12}\text{@As}_{20}$ complex. The isolated As_{20} is stable with a large HOMO-LUMO gap of 1.44 eV. In $\text{As@Ni}_{12}\text{@As}_{20}$, Ni d minority spin states are filled and the LUMO have a predominantly p character. An analysis of the atom projected DOS and the orbital densities shows that both the HOMO and LUMO are centered around the Ni atoms. Our calculation on -1 and -2 charged states show that the isolated molecule is most stable in the -2 charged state. Although the electronic states are completely filled in the triply charged anion, the electrostatic repulsion due to the extra electrons makes the molecule energetically unfavorable in the gas phase. The first and second electron affinities of the $\text{As@Ni}_{12}\text{@As}_{20}$ are 3.47 and 0.74 eV respectively. The accuracy of the electron affinities is subject to the exchange-correlation functional used [11]. The low binding energy of the second electron makes it susceptible to detachment in the laser desorption experiments. This is consistent with the observation that the mass spectrum shows peaks for the singly charged anions [5].

To determine qualitatively the nature of bonding between Ni and the As shell, we have integrated the charge density inside non-overlapping spheres of arbitrary radii around each atom. These values in units of e are given in Table II and show a very small amount of charge transfer upon formation of the onion-like molecule especially around the outer shell As atoms. The same feature is seen in various charged states of the molecule. There could be two possible causes for the small charge transfer between the atoms. First, the interaction between the As_{20} and As@Ni_{12} cages may be weak and secondly, the environment around the outer As atoms may be similar in As_{20} and in $\text{As@Ni}_{12}\text{@As}_{20}$.

The strength of interaction between the two cages will also be reflected in the vibrational modes of $\text{As@Ni}_{12}\text{@As}_{20}$ and its infrared (IR) and Raman activity. If the bonding between the cages is weak, then the vibrational modes of the $\text{As@Ni}_{12}\text{@As}_{20}$ will be quite similar to those of isolated As_{20} and As@Ni_{12} .

The vibrational frequencies for $\text{As@Ni}_{12}\text{@As}_{20}$ and both of its sub-units are real indicating that they are vibrationally stable. The vibrational frequencies of this massive molecule range between 42 to 305 cm^{-1} . The frequencies of the As_{20} and As@Ni_{12} range from 63 – 248 cm^{-1} and from 104 – 305 cm^{-1} , respectively. The mean polarizability of $\text{As@Ni}_{12}\text{@As}_{20}$ is 25.7 bohr³ per atom which indicates that this molecule may be useful for application in optical devices. From the polarizability to molecular volume ratio, we find that the polarizability

TABLE I: The experimental and calculated values of bond lengths are presented in Å. Note that (c) refers to the central As atom. The eigenvalues of the HOMO and the LUMO levels are given in Hartrees. The last column shows the Hubbard U parameter in Hartree/electron².

Method	As - As	Ni - Ni	As - Ni	As(c) - Ni	E_{HOMO}	E_{LUMO}	U
Expt.	2.75		2.40	2.56			
As ₂₀	2.50				-0.1974	-0.1443	0.1052
As@Ni ₁₂		2.48		2.36	-0.1445	-0.1384	0.1266
As@Ni ₁₂ @As ₂₀	2.80	2.74	2.43	2.61	-0.1827	-0.1789	0.1029
[As@Ni ₁₂ @As ₂₀] ⁻³	2.80	2.72	2.44	2.59			

of the As@Ni₁₂@As₂₀ is about 10% larger than in C₆₀ molecule. The IR absorption (top three panels) and the Raman spectra (bottom three panels) of As@Ni₁₂@As₂₀ together with its isolated sub-units are presented in Fig. 3. The projection of the spectra of As@Ni₁₂@As₂₀ on the As and Ni cages are also shown in the same figure. The As@Ni₁₂@As₂₀ has ten optical modes - four IR and six Raman active modes. These modes and their corresponding symmetries are tabulated in Table III.

The triply degenerate IR active modes belong to the T_{1u} symmetry. The IR spectrum of As@Ni₁₂@As₂₀ is dominated by a large peak at 265 cm⁻¹ with three smaller peaks at 84, 163, and 212 cm⁻¹. The As₂₀ cage shows little IR activity with a single peak at 167 cm⁻¹ which disappears upon encapsulation. The low frequency IR mode of As@Ni₁₂@As₂₀ at 84 cm⁻¹ appears to be due to the rocking motion of the As@Ni₁₂ in which the As₂₀ cage also gets mildly distorted. This rocking motion is also responsible for the peak seen at 143 cm⁻¹ in the IR spectra of As@Ni₁₂. The small peak at 163 cm⁻¹ in the IR of As@Ni₁₂@As₂₀ is due to the motion of the central As atom. The most dominant peak in the spectrum of As@Ni₁₂@As₂₀ at 265 cm⁻¹ is caused by torsional motion mostly of the Ni cage. This peak can not be correlated with the peak at 305 cm⁻¹ in the As@Ni₁₂ spectra.

The Raman active modes have A_{1g} and H_g symmetry which are one and five-fold degenerate. The lowest modes of the As₂₀ and As@Ni₁₂ couple and form the two peaks at 67 cm⁻¹ and 102 cm⁻¹ upon encapsulation. The increased intensity of the lowest Raman peak is a result of increase in polarizability derivative upon encapsulation. In fact, we find that the ratio of the Raman scattering intensities of As@Ni₁₂@As₂₀ and As₂₀ scales *exactly* as the square of the ratio of their radii. Similar agreement between the intensities and the ratios of the radii is also observed for As@Ni₁₂@As₂₀ and As@Ni₁₂.

TABLE II: The charge within a sphere of radius 2.28 a.u. and 2.17 a.u. around the As and Ni atoms, respectively. The symbols (c) and (s) refer to the central and outer shell.

Complex	Ni	As(c)	As(s)
As ₂₀			31.06
As@Ni ₁₂	26.76	31.46	
As@Ni ₁₂ @As ₂₀	26.90	31.10	31.05

These modes are 5-fold symmetric involving stretching of the molecule diameter. The mode at 142 cm⁻¹ is a breathing mode and correlates to the breathing mode of As₂₀ at 152 cm⁻¹. The As@Ni₁₂ shows a Raman peak due to breathing motion at 263 cm⁻¹. This mode and the breathing mode of the As₂₀ cage at 152 cm⁻¹ couple together to form a peak at 227 cm⁻¹ which is basically an asynchronous breathing motion with motions of the Ni and As cage being in opposite phase.

The absence of a one-to-one mapping between the vibrational modes of As@Ni₁₂@As₂₀ and its sub-units in the IR and Raman spectra indicates that the interaction between these sub-units is non-negligible. We do not see any pure “rattling” motion of As@Ni₁₂ inside the As₂₀ cage. On the contrary, there seems to be a strong coupling of the vibrational modes between the As@Ni₁₂ and the As₂₀ cages.

The same feature of strong interaction is also seen in the isodensity surfaces of the As@Ni₁₂@As₂₀ cluster. In Fig. 4, we present the isovalued surfaces of charge density in the isolated As₂₀ and in the encapsulated As@Ni₁₂@As₂₀ cluster. The density surface in As₂₀ shows covalent bonding between the As atoms. The As atoms in As₂₀ are sp³ hybridized and form covalent σ -bonds with its three nearest As neighbours. The fourth orbital contains a lone pair of electrons pointing radially outward. However, in the encapsulated form, each of the outer As atoms have three nearest neighbor Ni atoms and form strong covalent bonds with the *Ni d orbitals rather than with other As atoms*. We refer to this phenomenon as rebonding of the As atoms. Thus each As atom has 8 surrounding valence electrons and each of the Ni atoms form such covalent bonds with its five nearest As atoms. The Ni atoms occupy a position near the center of the pentagonal faces but slightly out of plane and since the As-Ni bonds are stronger than Ni-Ni bonds, the Ni cage expands. The expansion of the As cage occurs possi-

TABLE III: The IR and Raman active frequencies of As@Ni₁₂@As₂₀. The values are in cm⁻¹.

Symmetry	Frequency
A _{1g}	142, 227
T _{1u}	84, 163, 212, 265
H _g	67, 101, 177, 297

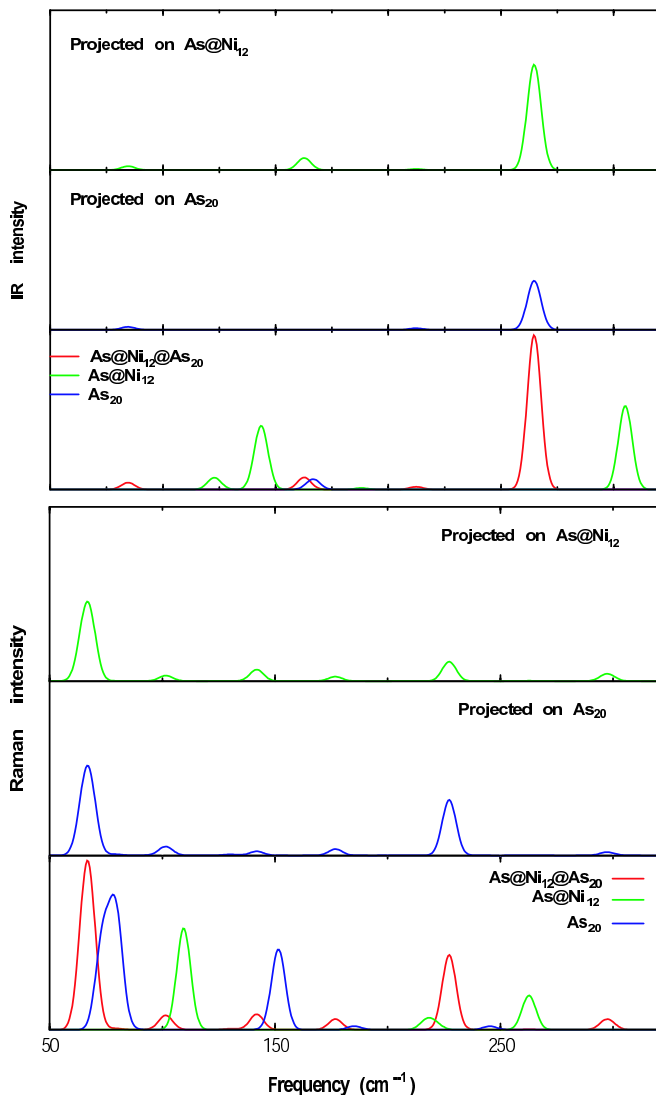


FIG. 3: The IR and Raman spectra for the $\text{As@Ni}_{12}@As_{20}$ molecule and its sub-units (see text for details).

bly due to the kinetic energy repulsion. It may be mentioned here that the most favorable dissociation channel for isolated As_{20} is As_4 [10] whereas the laser desorption

mass spectroscopy shows peaks for all $\text{As@Ni}_{12}@As_x$ for $x=1,20$ [5]. Since in the encapsulated structure, each As is now bonded strongly with three nearest Ni atoms and the As-As bonds are much weaker than in As_{20} , the laser desorption experiment breaks away each As atom individually rather than in As_4 .

In conclusion, we find that the isolated $\text{As@Ni}_{12}@As_{20}$ cluster has I_h symmetry and is vibrationally stable. We find that the molecule will be electronically stable in the -3 charged state in the condensed phase due to the opening of a large HOMO-LUMO gap. The electrostatic repulsion makes it more stable in the -2 charged state when in the gas phase. Our analysis of the IR and Raman spectra of the molecule *vis-à-vis* its sub-units and the electronic structure shows that the outer cage As

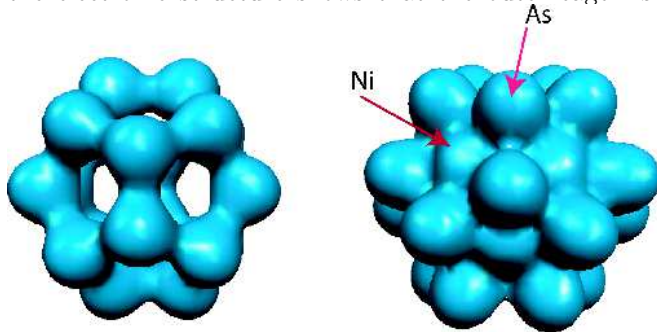


FIG. 4: The iso-surface of the total charge density in As_{20} and in $\text{As@Ni}_{12}@As_{20}$ cluster.

As bonding changes dramatically upon encapsulation of As@Ni_{12} . There exists strong covalent bonding between the outer As atoms and inner Ni atoms, in contrast to the Huckel-based prediction of Ref. 5. Our study provides an understanding of the bonding and will be useful for further experimental characterization.

TB and MRP acknowledge financial support from ONR (Grant No. N000140211046) and by the DoD High Performance Computing CHSSI Program. RRZ thanks GMU for support and SLR is grateful for financial support as a Distinguished Summer Faculty Fellow in the ONR-American Society for Engineering Education Summer Faculty Program.

-
- [1] H. W. Kroto *et al.*, Nature (London) **318**, 162 (1985).
 [2] W. Kratschmer *et al.*, Nature (London) **347**, 254 (1990).
 [3] B. C. Guo *et al.* Science **255**, 1412 (1992); G. K. Gueorguiev and J. M. Pacheco, Phys. Rev. Lett. **88**, 115504 (2002); T. Baruah *et al.*, Phys. Rev. A **66**, 053201 (2002).
 [4] H. Hiura *et al.*, Phys. Rev. Lett. **86**, 1733 (2001); S.N. Khanna *et al.*, Phys. Rev. Lett. **89**, 016803 (2002); L. Mitas *et al.*, Phys. Rev. Lett. **84**, 1479 (2000); S. C. Sevov and J. D. Corbett, Science **252**, 880 (1993).
 [5] M. J. Moses *et al.* Science **300**, 778 (2003).
 [6] G. Bergman *et al.* Acta Cryst. **10**, 254 (1957).
 [7] A. Müller, Science **300**, 749 (2003).
 [8] J. P. Perdew *et al.* Phys. Rev. Lett. **77**, 3865(1996).
 [9] M. R. Pederson and K. A. Jackson, Phys. Rev. B. **41**, 7453 (1990); *ibid* **43**, 7312 (1991); K. A. Jackson and M. R. Pederson, *ibid* **42**, 3276 (1990).
 [10] M. Shen and H. F. Schaefer, J. Chem. Phys., **101**, 2261 (1994).
 [11] J. C. Rienstra-Kiracofe *et al.* Chem. Rev. **102**, 231 (2002).